M. M. Kesavulu
A. S. Prakasha Gowda
T. N. C. Ramya
N. Surolia
K. Suguna

Plasmepsin inhibitors: design, synthesis, inhibitory studies and crystal structure analysis

Authors' affiliations:
M. M. Kesavulu, A. S. Prakasha Gowda, T. N. C. Ramya and K. Suguna Molecular Biophysics Unit, Indian Institute of Science, Bangalore, India

N. Surolia, Jawaharlal Nehru Centre for Advanced Scientific Research, Jakkur, Bangalore, India

Correspondence to:
K. Suguna
Molecular Biophysics Unit
Indian Institute of Science
Bangalore – 560012
Karnataka, India
Tel.: 91 80 22932838
Fax: 91 80 23600535
E-mail: suguna@mbu.iisc.ernet.in

Key words: malaria; plasmepsins; *Plasmodium falciparum*; plasmepsin inhibition; aspartic protease

Abstract: Plasmepsin group of enzymes are key enzymes in the life cycle of malarial parasites. As inhibition of plasmepsins leads to the parasite's death, these enzymes can be utilized as potential drug targets. Although many drugs are available, it has been observed that *Plasmodium falciparum*, the species that causes most of the malarial infections and subsequent death, has developed resistance against most of the drugs. Based on the cleavage sites of hemglobin, the substrate for plasmepsins, we have designed two compounds (*p*-nitrobenzoyl-leucine-β-alanine and *p*-nitrobenzoyl-leucine-isonipecotic acid), synthesized them, solved their crystal structures and studied their inhibitory effect using experimental and theoretical (docking) methods. In this paper, we discuss the synthesis, crystal structures and inhibitory nature of these two compounds which have a potential to inhibit plasmepsins.

Abbreviations: DCC, dicylohexyl carbodiamide; HAP, histo-asparstic protease; Hb, hemoglobin; HOBt, 1-hydroxybenzotrizole.

Introduction

Every year, billions of people are infected with malaria and close to 3 million people die because of the disease (1). Malaria is caused by four major species, *Plasmodium falciparum*, *P. vivax*, *P. malariae*, and *P. ovale*. Among these four major species, *P. falciparum* alone accounts for more than 95% of the malaria cases (2). Although many antimalarial drugs are available, both *P. falciparum* and *P. vivax* have developed resistance for almost all the available drugs (3,4). Therefore, to find newer antimalarial agents is indeed the need of the hour.

The asexual development of the malarial parasite takes place in human erythrocyte or the red blood cell (RBC).

During this stage, the parasite utilizes hemoglobin (Hb) of RBC as the only source of food. Three different classes of enzymes present in the food vacuole of the malarial parasite – falcipain (cysteine protease) (5), falcilysin (metalloprotease) (6) and plasmepsins (aspartic proteases) (7) – are responsible for the digestion of Hb. Of the three different classes of enzymes involved in the digestion of Hb, plasmepsins are known to be the key enzymes as they initiate the catalytic breakdown of Hb. Hence, these enzymes can be probed as potential drug targets. Three aspartic proteases (plasmepsin I, II and IV) and one histo-aspartic protease (HAP) are involved in Hb degradation (8,9). Plasmepsins I and II are involved in the first phase of Hb degradation, while plasmepsin IV and HAP either partially digest Hb or act on the degradation products of the first phase to cleave them into smaller peptides. Recent genome data of *P. falciparum* revealed the presence of six more plasmepsins (plasmepsins V to X) in the parasite. These enzymes share much less similarity among themselves and with the other four aspartic proteases and their functions are not yet known.

Since the identification of plasmepsins in 1994 (10), numerous attempts have been made to design inhibitors of plasmepsins with a view to develop them into potent antimalarial drugs. A wide variety of them have been designed, synthesized, checked for activity by enzyme assays as well as in parasite cultures. They include both peptide-like (7,11,12) and non-peptidyl (4,13,14) inhibitors. Some of them were designed based on the substrate structure (Phe33-Leu34 of Hb) (15) and/or statine residue (16) of the universal aspartic protease inhibitor, pepstatin. C2 symmetric (17) and achiral inhibitors (4) were also reported. The determination of the crystal structure of plasmepsin II in complex with pepstatin revealed intricate details of the mode of binding and provided a platform for the structure-based design (18). Subsequent crystal structures of plasmemsin II with other inhibitors (13,15) revealed the conformational flexibility of the binding pocket and an entirely new type of binding (19). Modeling/docking, molecular dynamics and interaction energy calculations were also performed in many studies (4,17). Some of the compounds could successfully inhibit the enzyme but failed to stop the parasite growth in cell culture (4,7,18) probably because of their size that prevents the access to the food vacuole of the parasite where the Hb degradation occurs. The strategy for a viable drug is to find a relatively small, cost-effective and highly specific inhibitor. Although many inhibitors targeting the plasmepsin group of enzymes are available, none of them are in use as drugs for the treatment of malaria today. We have designed and

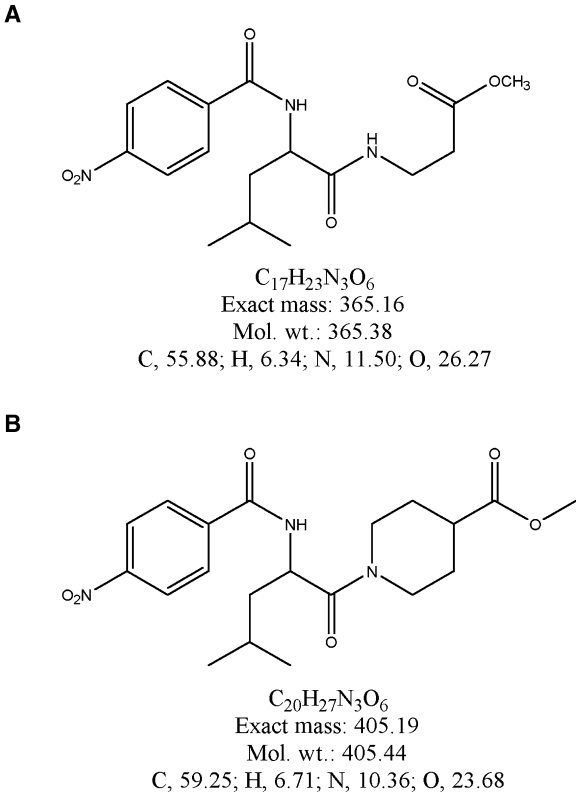

Figure 1. Chemical structures of (A) *p*-nitrobenzoyl-leucine-β-alanine (Asp-12) and (B) *p*-nitrobenzoyl-leucine-isonipecotic acid (Asp-20).

synthesized two small compounds (Fig. 1) based on the Hb cleavage sites of plasmepsins and also incorporated a β-amino acid in one of them and the isonipecotic acid group in the other as alternate strategies for inhibitor design with a view to test the feasibility of developing them as effective antimalarials. To study the interaction of these compounds with plasmepsin I, we have crystallized both the compounds, determined their crystal structures and performed docking studies using the crystal structures, the results of which are presented in this paper.

Experimental Procedures

Synthesis of compounds

The compounds were synthesized by the stepwise solution-phase method. Dicyclo hexylcarbodiamide (DCC) was used for the formation of the peptide bond.

p-(NO_2)-Ba-(L),(D)-Leu-β-Ala-OMe (Asp-12 & Asp-13)

p-(NO_2)-Ba-(L)-Leu-OH or *p*-(NO_2)-Ba-(D)-Leu-OH (0.9 g, 3.21 mM) was dissolved in 10 mL of ethyl acetate and cooled to 0 °C in an ice bath. H-β-Ala-OMe, isolated from

Table 1. **Details of crystal data, data collection and refinement parameters**

	Asp-12/Asp-13	Asp-20/Asp-21
Empirical formula	$C_{17}H_{23}N_3O_6$	$C_{20}H_{27}N_3O_6$
Crystal size (mm)	0.44 × 0.19 × 0.09	0.2 × 0.17 × 0.1
Crystallizing solvent	Acetone	Acetone
Crystal system	Triclinic	Monoclinic
Space group	P 1	C 1 2/c 1
Unit cell dimensions		
a (Å)	8.791(3)	17.246(4)
b (Å)	9.725(3)	12.800(3)
c (Å)	11.165(4)	19.708(4)
α (°)	92.231(6)	90
β (°)	95.723(6)	96.138(5)
γ (°)	98.977(6)	90
Volume (Å^3)	936.7(13)	4325.36(29)
Z	2	8
Mr	365.4	405.5
Density (g/cm^3) (cal)	1.3	1.25
F(000)	387.9	1727.7
Radiation (λ in Å)	MoKα (0.71073)	MoKα (0.71073)
Temperature (°C)	20	25
Unique reflections	3913	2278
Observed reflections	3023	1374
Final R (%)	3.63	6.76
Final wR2 (%)	7.56	14.62
Goodness of fit (S)	0.957	1.009
$\Delta\rho_{max}$ (e Å^{-3})	0.120	0.428
$\Delta\rho_{min}$ (e Å^{-3})	−0.093	−0.154
Data-to-param ratio	8.2:1	8.5:1

0.7 g (6.42 mM, 2 eq.) of hydrochloride was neutralized, followed by extraction with ethyl acetate and concentration to approximately 5 mL. It was then added to *p*-(NO_2)-Ba-Leu-OH under stirring while maintaining the temperature at 0 °C, followed immediately by the addition of DCC/1-hydroxybenzotrizole (HOBt) of 0.70 g (3.21 mM)/0.43 g (3.21 mM). The reaction mixture was allowed to reach room temperature and stirred for 3–4 h. The precipitated dicyclohexylurea was filtered off. The organic layer was washed successively with 2 N HCl (3 × 50 mL), brine (3 × 50 mL), 1 M sodium carbonate (3 × 50 mL) and brine (3 × 50 mL). This layer was then dried over anhydrous sodium sulfate and was evaporated to yield a white solid. The crude peptide was recrystallized from petroleum ether to obtain Asp-12/Asp-13. The sample was purified over silica gel using chloroform–methanol as an elutant to yield 0.96 g (2.63 mM, 82.10%) of Asp-12/Asp-13.

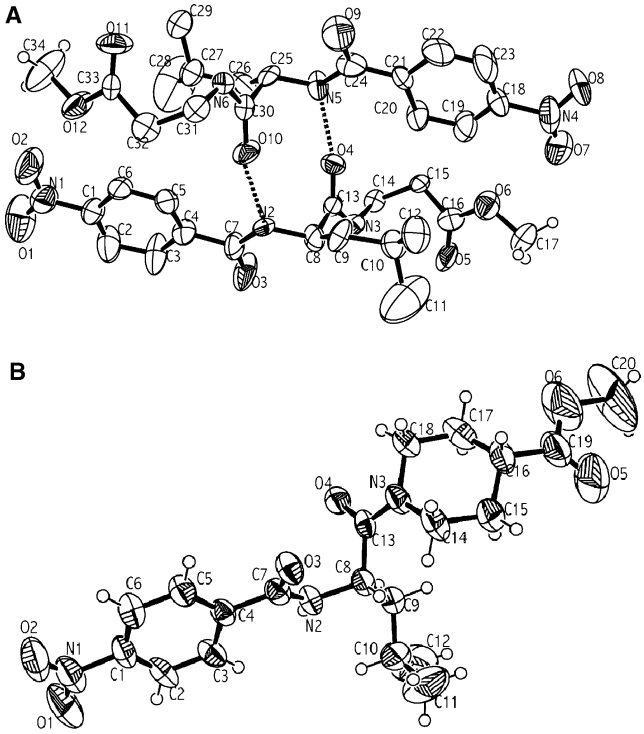

Figure 2. Molecular conformation of (A) Asp-12 & Asp-13 and (B) Asp-20. The thermal ellipsoids are at 50% probability level.

p-(NO_2)-Ba-(L),(D)-Leu-Ina-OMe (Asp-20 & Asp-21)

p-(NO_2)-Ba-(L)-Leu-OH or *p*-(NO_2)-Ba-(D)-Leu-OH (0.28 g, 1.0 mM) was dissolved in 5 mL of ethyl acetate and cooled to 0 °C in an ice bath. H-Ina-OMe (Ina-isonipecotic acid), isolated from 0.28 g (2.0 mM, 2 eq.) of hydrochloride was neutralized, followed by extraction with ethyl acetate, and concentration to approximately 5 mL. It was then added to *p*-(NO_2)-Ba-Leu-OH under stirring while maintaining the temperature at 0 °C, followed immediately by the addition of DCC/HOBt of 0.21 g (1.0 mM)/0.14 g (1.0 mM). The reaction mixture was allowed to reach room temperature and stirred for 3–4 h. The precipitated dicyclohexylurea was filtered off. The organic layer was washed successively with 2 N HCl (3 × 50 mL), brine (3 × 50 mL), 1 M sodium carbonate (3 × 50 mL) and brine (3 × 50 mL). This layer was then dried over anhydrous sodium sulfate and was evaporated to yield a white solid. The crude peptide was recrystalized from petroleum ether to obtain Asp-20/Asp-21. The sample was purified over silica gel using chloroform–methanol as an elutant to yield 0.35 g (0.86 mM, 86.30%) of Asp-20/Asp-21.

Characterization

Elemental analysis of the compounds was carried out using a ThermoFinnigan FLASH EA 1112 CHNS analyser (Thermo Electron Corporation, Waltham, MA, USA) and the

Table 2. **Coordinates and equivalent isotropic thermal parameters (× 10^3 Å^2) of nonhydrogen atoms (estimated standard deviations are given in parentheses)**

Asp-12				
O1	−0.5067 (0.0070)	−1.4406 (0.0067)	1.5154 (0.0061)	1060 (30)
O2	0.1822 (0.0071)	0.0081 (0.0063)	0.0504 (0.0058)	1189 (29)
N1	0.0890 (0.0071)	−0.4805 (0.0076)	1.1807 (0.0074)	886 (31)
C1	0.7506 (0.0075)	0.2754 (0.0072)	2.3204 (0.0075)	578 (30)
C2	0.6096 (0.0077)	−0.1022 (0.0055)	3.5786 (0.0069)	702 (30)
C3	1.2293 (0.0071)	0.6880 (0.0068)	4.6132 (0.0063)	585 (27)
C4	1.9832 (0.0064)	1.7183 (0.0061)	4.2803 (0.0064)	480 (23)
C5	2.1786 (0.0071)	2.0284 (0.0083)	2.9870 (0.0075)	804 (32)
C6	1.5215 (0.0087)	1.2953 (0.0098)	1.9448 (0.0075)	922 (40)
C7	2.7881 (0.0062)	2.4696 (0.0067)	5.3023 (0.0064)	578 (31)
O3	3.5516 (0.0059)	3.3398 (0.0056)	4.9106 (0.0056)	957 (23)
N2	2.6303 (0.0055)	2.2322 (0.0053)	6.5935 (0.0048)	572 (23)
C8	3.4035 (0.0064)	2.9187 (0.0063)	7.6185 (0.0064)	627 (27)
C9	2.6750 (0.0068)	3.0248 (0.0085)	8.8924 (0.0074)	797 (33)
C10	3.4081 (0.0069)	3.7288 (0.0064)	10.0557 (0.0058)	600 (26)
C11	2.5807 (0.0102)	3.5924 (0.0098)	11.3526 (0.0083)	1007 (39)
C12	3.7013 (0.0093)	5.2028 (0.0074)	9.8164 (0.0087)	1000 (40)
C13	4.7541 (0.0059)	2.2119 (0.0063)	7.7960 (0.0054)	373 (23)
O4	4.8284 (0.0040)	1.0535 (0.0044)	8.1494 (0.0040)	541 (18)
N3	5.8411 (0.0047)	2.9984 (0.0050)	7.5924 (0.0049)	467 (20)
C14	7.2394 (0.0058)	2.4862 (0.0066)	7.7391 (0.0063)	533 (22)
C15	7.5627 (0.0063)	2.4046 (0.0059)	9.2402 (0.0063)	452 (25)
C16	7.5353 (0.0068)	3.7258 (0.0072)	9.9451 (0.0073)	561 (30)
O5	7.6104 (0.0057)	4.7796 (0.0050)	9.3857 (0.0053)	795 (23)
O6	7.4462 (0.0053)	3.6019 (0.0047)	11.2404 (0.0050)	744 (21)
C17	7.4488 (0.0113)	4.8222 (0.0094)	12.0421 (0.0094)	1386 (52)
Asp-13				
O7	5.6127 (0.0067)	1.1787 (0.0074)	15.8850 (0.0064)	1248 (31)
O8	6.3195 (0.0065)	2.5602 (0.0061)	14.4591 (0.0063)	1104 (28)
N4	5.6861 (0.0069)	1.5165 (0.0075)	14.7451 (0.0060)	731 (30)
C18	5.0287 (0.0072)	0.7412 (0.0073)	13.7249 (0.0068)	567 (29)
C19	5.1982 (0.0064)	1.1325 (0.0070)	12.4067 (0.0068)	730 (31)
C20	4.5564 (0.0080)	0.4735 (0.0071)	11.4689 (0.0071)	725 (32)
C21	3.7138 (0.0066)	−0.6545 (0.0070)	11.7126 (0.0068)	570 (29)
C22	3.6911 (0.0096)	−1.0572 (0.0095)	13.0638 (0.0083)	1028 (39)
C23	4.2925 (0.0099)	−0.3978 (0.0094)	14.0296 (0.0089)	946 (37)
C24	2.9622 (0.0077)	−1.4539 (0.0061)	10.7227 (0.0070)	647 (32)
O9	2.1712 (0.0060)	−2.3257 (0.0063)	11.0692 (0.0051)	1044 (27)
N5	3.1430 (0.0049)	−1.1632 (0.0046)	9.4130 (0.0053)	501 (21)
C25	2.3376 (0.0059)	−1.8784 (0.0053)	8.4144 (0.0053)	430 (22)
C26	3.1129 (0.0063)	−1.9559 (0.0059)	7.0886 (0.0063)	507 (25)
C27	2.3997 (0.0069)	−2.6978 (0.0066)	5.9524 (0.0073)	627 (31)
C28	3.2062 (0.0097)	−2.5632 (0.0092)	4.6998 (0.0083)	991 (35)
C29	2.1428 (0.0086)	−4.1365 (0.0071)	6.2802 (0.0072)	849 (32)
C30	1.0169 (0.0071)	−1.1951 (0.0068)	8.2192 (0.0060)	500 (27)
O10	0.9483 (0.0040)	0.0211 (0.0040)	7.8431 (0.0042)	549 (18)

Table 2. **Continued**

N6	−0.0526 (0.0054)	−1.8982 (0.0047)	8.4361 (0.0050)	476 (21)
C31	−1.3601 (0.0065)	−1.4275 (0.0055)	8.2055 (0.0061)	463 (23)
C32	−1.7958 (0.0074)	−1.3366 (0.0066)	6.7547 (0.0066)	569 (29)
C33	−1.7847 (0.0060)	−2.6770 (0.0070)	6.0996 (0.0067)	493 (26)
O11	−1.8240 (0.0056)	−3.7593 (0.0049)	6.6511 (0.0053)	770 (24)
O12	−1.7382 (0.0051)	−2.5364 (0.0046)	4.7605 (0.0049)	725 (22)
C34	−1.7024 (0.0078)	−3.7538 (0.0074)	3.9848 (0.0071)	749 (32)
Asp-20				
O4	−0.7270 (0.0031)	0.1389 (0.0038)	11.8792 (0.0031)	559 (14)
O3	−3.1508 (0.0031)	−2.2724 (0.0035)	11.8319 (0.0035)	580 (14)
N2	−1.8218 (0.0043)	−1.7139 (0.0042)	10.1143 (0.0049)	494 (17)
N3	−0.1124 (0.0040)	−1.5201 (0.0045)	13.2575 (0.0043)	555 (17)
C4	−4.2251 (0.0050)	−1.5985 (0.0045)	9.8276 (0.0055)	462 (20)
C1	−6.5243 (0.0057)	−1.2527 (0.0049)	8.3882 (0.0069)	582 (25)
O2	−8.8317 (0.0049)	−1.0625 (0.0046)	8.2334 (0.0055)	1070 (23)
C7	−3.0131 (0.0052)	−1.8811 (0.0049)	10.6790 (0.0059)	482 (22)
C9	0.6009 (0.0047)	−1.8893 (0.0050)	10.0212 (0.0049)	556 (23)
C8	−0.6291 (0.0045)	−2.0125 (0.0049)	10.9002 (0.0047)	483 (22)
C2	−5.3693 (0.0061)	−1.4853 (0.0052)	7.7225 (0.0055)	621 (22)
N1	−7.7766 (0.0063)	−1.0992 (0.0054)	7.5989 (0.0073)	851 (29)
C5	−5.4213 (0.0057)	−1.3463 (0.0051)	10.4597 (0.0055)	621 (24)
C13	−0.5101 (0.0045)	−1.0645 (0.0061)	12.0655 (0.0053)	448 (21)
C3	−4.2171 (0.0052)	−1.6636 (0.0049)	8.4473 (0.0055)	578 (23)
C6	−6.5868 (0.0056)	−1.1759 (0.0054)	9.7523 (0.0067)	678 (26)
C18	0.2201 (0.0054)	−0.5858 (0.0056)	14.3283 (0.0051)	661 (24)
C16	2.1215 (0.0050)	−2.0873 (0.0063)	14.9781 (0.0053)	670 (25)
C17	1.6925 (0.0056)	−0.6754 (0.0064)	14.6389 (0.0053)	756 (27)
C14	0.1960 (0.0054)	−2.8947 (0.0058)	13.6053 (0.0055)	717 (26)
O1	−7.6832 (0.0049)	−1.0464 (0.0054)	6.4075 (0.0059)	1208 (22)
O6	4.0867 (0.0051)	−1.2391 (0.0070)	15.8755 (0.0067)	1573 (35)
C11	0.8276 (0.0090)	−4.1912 (0.0078)	9.0855 (0.0082)	1591 (49)
C15	1.6636 (0.0056)	−3.0613 (0.0058)	13.8919 (0.0055)	751 (27)
O5	4.1745 (0.0057)	−3.2673 (0.0083)	15.1141 (0.0067)	1756 (37)
C10	0.6738 (0.0061)	−2.7537 (0.0069)	8.7846 (0.0059)	810 (30)
C19	3.5909 (0.0078)	−2.2182 (0.0120)	15.2534 (0.0074)	1164 (46)
C12	1.7923 (0.0080)	−2.2473 (0.0091)	7.8728 (0.0073)	1517 (47)
C20	5.5308 (0.0075)	−1.3150 (0.0132)	16.1502 (0.0102)	2452 (79)

composition was confirmed (Asp-12: $C_{17}H_{23}N_3O_6$ and Asp-20: $C_{20}H_{27}N_3O_6$). Mass of the compounds was determined by electronspray mass spectrometry (Asp-12: $M_{cal} = 365.4$, $M_{obs} = 366.2$; Asp-20: $M_{cal} = 405.5$, $M_{obs} = 404.3$). The purity of the compounds was confirmed by thin-layer chromatography (TLC) by spotting them on silica gel 60 plates and developing with the following solvent systems: (1) chloroform:methanol:acetic acid 9:3:1 and (2) hexane:ethyl acetate 13:7. High-pressure liquid chromatography was performed by injecting the samples into a C18 reverse-phase column (4.6 × 150 mm, 5 μm) and eluting with acetonitrile. Single peaks (retention time 4.62 min for Asp-12 and 3.49 min for Asp-20) were detected with absorbance detector at 230 nm). The melting points were found to be between 118 and 119 °C for both the compounds.

The ^{1}H-nuclear magnetic resonance (NMR) spectra were recorded in $CDCl_3$ and the ^{13}C-NMR spectra were recorded in dimethyl sulfoxide (DMSO)-d_6 with 400 MHz Bruker

Table 3. **Hydrogen bonds**

	N…O distance (Å)	∠N–H…O (°)	Symmetry		
Intramolecular (Asp-12/Asp-13)					
N2…O10	3.046	165.3			
N5…O4	3.058	165.7			
Intermolecular (Asp-12/Asp-13)					
N3…011	3.026	175.5	$x + 1$	$y + 1$	z
N6…05	3.103	176.1	$x - 1$	$y - 1$	z
Intermolecular (Asp-20)					
N2…04	2.903	172.0	$-x$	$-y$	$-z + 1$

DRX instrument (Bruker Biospin Corporation, Billerica, MA, USA) at 25 °C. For Asp-12 ^{1}H-NMR: δ 8.18 (2H aryl), δ 7.92 (2H aryl), δ 7.5 (1H amido),δ 6.92 (1H amido), δ 4.65 (1H CH), δ 3.67, 3.51 (2H CH_2 leucyl side chain), δ 2.53, 2.03 (2H CH_2-CH_2), δ 1.87, 1.69 (4H CH_2CH_2), δ 0.93 (6H terminal methyl of leucyl side chain); ^{13}C NMR: δ 171.97 (amide), δ 171.75 (carboxyl), δ 164.81 (amide), δ 149.12 (aryl), δ 139.88 (aryl), δ 129.08 (aryl), δ 123.38 (aryl), δ 52.14 (aliphatic), δ 51.33 (aliphatic), δ 40.47 (aliphatic), δ 40.18 (aliphatic), δ 39.98 (aliphatic), δ 39.77 (aliphatic), δ 39.56 (aliphatic), δ 39.35 (aliphatic), δ 38.95 (aliphatic), δ 34.9(aliphatic), δ 33.62(aliphatic), δ 24.48 (aliphatic), δ 22.96 (aliphatic), δ 21.49 (aliphatic) and for Asp-20 ^{1}H-NMR: δ 8.35 (2H aryl), δ 8.19 (2H aryl), δ 4.54 (1H CH leucyl residue), δ 3.67 (3H CH_3 terminal methyl), δ 3.34 (2H piperidine), δ 2.33 (1H piperidine), δ 1.85 (2H piperidine), δ 1.83 (1H CH of leucyl side chain), δ 1.79 (1H CH_2 of leucyl side chain), δ 1.08 (6H CH_3 terminal methyl of leucyl side chain); ^{13}C-NMR: δ 177.1 (amido), δ 176 (carboxyl), δ 168 (amido), δ 152.1 (aryl), δ 139.8 (aryl), δ 128 (aryl), δ 123.5 (aryl), δ 51.5 (aliphatic), δ 50.8 (aliphatic), δ 43 (piperidine), δ 41.5 (piperidine), δ 37.8 (piperidine), δ 24.8 (aliphatic), δ 22.7 (aliphatic), δ 21.3 (aliphatic).

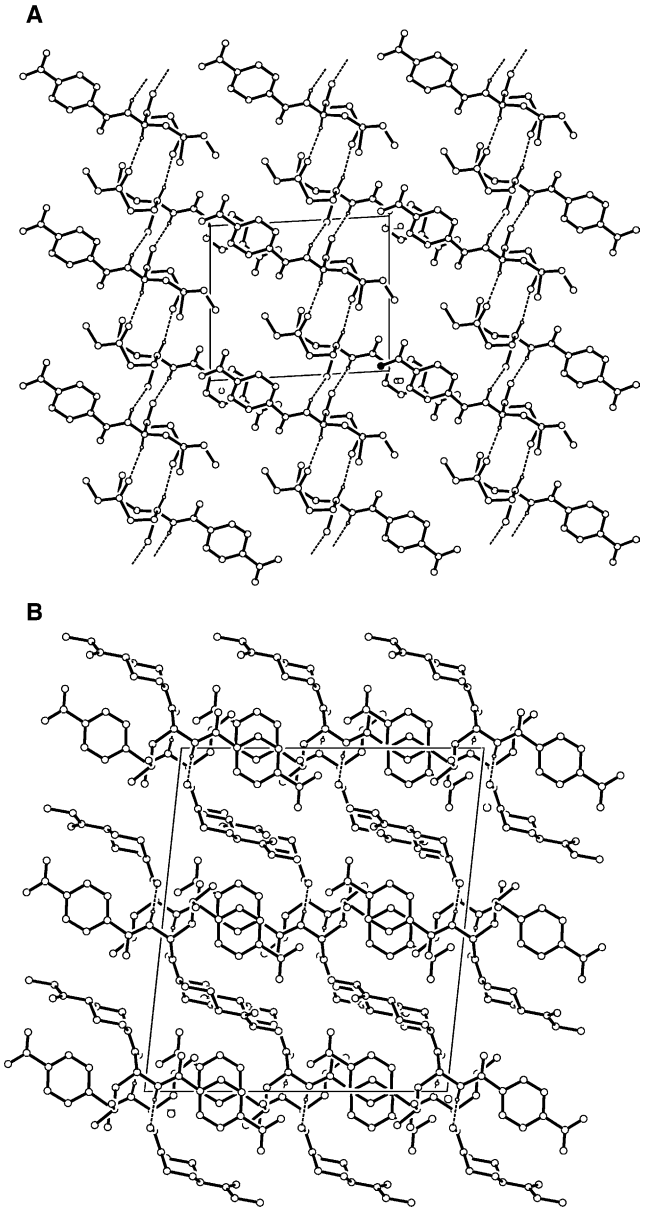

Figure 3. Crystal packing in (A) Asp-12 & Asp-13 and (B) Asp-20.

Assessment of inhibition of growth of *P. falciparum* cultures by peptides

Experiments requiring *Plasmodium* cultures used chloroquine-sensitive *P. falciparum* strain FCK2 (CQ-sensitive; IC_{50} 18 nM) parasites from Karnataka, India, cultivated in O+ human erythrocytes in medium supplemented with O+ human serum by the candle jar method of Trager and Jenson (20). Culture synchrony was maintained by 5% sorbitol treatment (21), and parasites were observed for viability and any changes in morphology by standard staining procedures (Giemsa staining).

Growth inhibition by the peptides of interest was assessed by monitoring the uptake of [^{3}H] hypoxanthine (22). Synchronized parasites in the early trophozoite stage were cultured in 96-well plates (Nunc, Copenhagen, Denmark) in

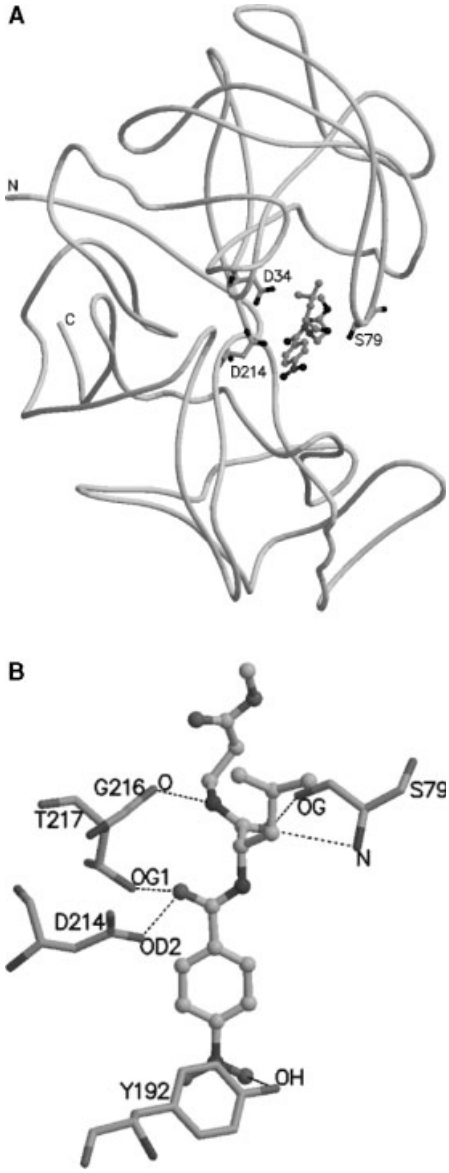

Figure 4. Results of molecular docking. (A) Asp-12 in the binding cleft of plasmepsin I. (B) Details of interactions between Asp-12 and plasmepsin I.

culture medium supplemented with 10% serum at 10% hematocrit and at an initial parasitemia of at least 3%. Different concentrations of the peptide in DMSO were added such that the final concentration of DMSO did not exceed 0.05%. Every peptide concentration was tested in triplicate. [^{3}H] hypoxanthine was added to the culture after incubation with peptide for 48 h and the cultures were further incubated for 31 h. The cultures from the wells of the plate were harvested using a Nunc cell harvester and inhibition of *P. falciparum* growth was assessed by measuring the incorporation of [^{3}H] hypoxanthine using a liquid scintillation counter (Wallac, Global Medical Instrumentation Inc, Ramsey, MN, USA). The relative percent parasitemia was plotted vs. log concentration of the inhibitor and the curve was fit to non-linear regression analysis using

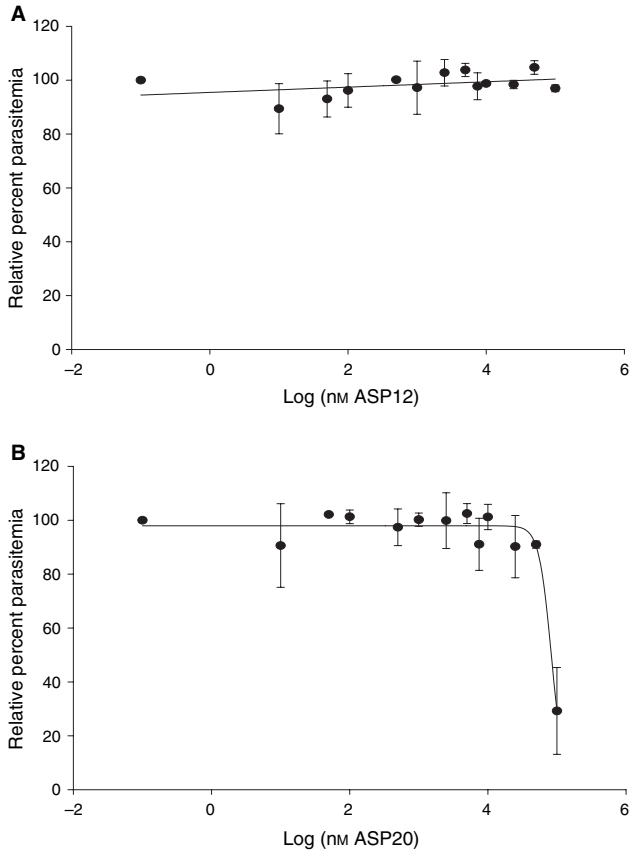

Figure 5. In vitro growth inhibition assay of the malaria parasite by the peptides (A) Asp-12 and (B) Asp-20.

SigmaPlot 2000 software (Systat Software Inc., Point Richmond, CA, USA). This allowed the calculation of IC_{50}.

Crystallization and data collection details

As Asp-12 was as inhibitory as Asp-13 and Asp-20 and Asp-21 are likewise equally active, saturated solutions of the equimolar mixtures of compounds (Asp-12/13 and Asp-20/21) were prepared in acetone as a solvent and the crystals were grown by slow evaporation of acetone at room temperature. Crystals grew in 7 days of crystallization setup. The X-ray data were collected on a Bruker AXS SMART APEX CCD diffractometer, using MoKα radiation ($\lambda = 0.71073$ Å). The structures were determined and refined using SHELXS-97 and SHELXL-97 (23), respectively.

Molecular modeling

As the initial cleavage of Hb is likely to be carried out by plasmepsin I, the structure of plasmepsin I modeled based on the coordinates of plasmepsin II [PDB code:1SME (18)] using

the program SYBYL (24) was used as a target for docking studies. The identity between the two plasmepsins (plasmepsins I and plasmepsin II) is 53.1%. The peptides Asp-12, Asp-13 and Asp-20, Asp-21 were docked into the modeled plasmepsin I with the program Autodock 3 (25), using the crystal structure coordinates of the peptides. Autodock 3 creates a grid box around the protein, pre-calculates the energy values at the grid points, randomly places ligand (inhibitors) and evaluates successive random changes in the position, orientation and conformational changes using a simulated annealing coupled with the metropolis energy test.

Results

Crystal structures

The details of crystal system and diffraction and refinement parameters of the two compounds are summarized in Table 1. The structures were determined by direct methods and the hydrogen atoms were located in difference Fourier maps. Anisotropic thermal parameters of the non-hydrogen atoms were refined in the final cycles of the refinement. Non-hydrogen atoms with their thermal ellipsoids are shown in Fig. 2.

The coordinates of non-hydrogen atoms with their equivalent isotropic thermal parameters are given in Table 2. Hydrogen bonds in the crystal structures are given in Table 3. Asp-12 and Asp-13 crystallize in space group P1 with one molecule each in the asymmetric unit. Two hydrogen bonds exist between these two molecules, made by the nitrogen and the carbonyl carbon atoms of the leucine residue. In addition, the molecules are stabilized in the lattice by two additional intermolecular hydrogen bonds (Table 3, Fig. 3). Asp-20 and Asp-21 crystallize in space group C2/c with one molecule in the asymmetric unit. Thus in the crystal Asp-20 and Asp-21 are related by the crystallographic symmetry. These two molecules are also held by intermolecular hydrogen bonds made between the nitrogen and the carbonyl oxygen atoms of the leucine residue (Table 3, Fig. 3).

Docking studies

Molecular docking of these four compounds into modeled plasmepsin I resulted in negative interaction energy with efficient binding. Hybrid search (global and adaptive local) of 50 cycles was carried out for all the four compounds.

We could dock all of them in the binding cleft of plasmepsin I. They block the active site by directly interacting with either one or both of the catalytic aspartates, Asp34 and Asp214 and also with Ser79 situated at the tip of the flexible 'flap' region. The interaction energies are in the range of −9 to −8 kcal/mol. The binding modes of one of them is shown in Fig. 4.

Inhibition of parasite growth

The inhibitory studies indicated no inhibition by Asp-12 & Asp-13 on *P. falciparum* cultures up to a concentration of 100 μM, while Asp-20 & Asp-21 inhibited the *P. falciparum* with an IC_{50} of 84 μM (Fig. 5).

Discussion

Degradation of Hb by enzymes present in the food vacuole of the malarial parasite is the key step for parasite's survival. Although three different classes of enzymes are involved in the Hb degradation process, plasmepsins play a major role in the initial degradation of Hb. These enzymes can be utilized as targets for drug development and discovery. There are many peptide like compounds such as pepstatin and others, which inhibit plasmepsins effectively, but their inhibitory action is limited only to plasmepsin enzymes and they do not show much effect on parasitic growth. This may be due to their longer chain size because of which they fail to gain entry into the parasite food vacuole, where Hb degradation takes place.

In our study we have used two compounds which are very small in size and effectively bind in the active site. The determination of their crystal structures enabled more accurate and faster docking calculations. Although docking studies showed that all the four compounds bind reasonably well at the active site with favourable energy, in contradiction to this, our experimental data showed only Asp-20/Asp-21 cause inhibition of parasite growth. The contradictory result of docking and experimental studies is due to the fact that docking is performed directly on the enzyme. Our experimental and computational results show that Asp-20/Asp-21 have a better potential to inhibit plasmepsins, whereas it is required to modify the design of Asp-12/Asp-13 to make them more effective as inhibitors of plasmepsins.

Acknowledgements: X-ray diffraction data were collected using the CCD diffractometer facility at the Indian Institute of Science supported by the IRPHA program of the Department of Science & Technology of India. The work was funded by the Council of Scientific and Industrial Research.

References

1. Breman, J.G., Alilio, M.S. & Mills, A. (2004) Conquering the intolerable burden of malaria: what's new, what's needed: a summary. *Am. J. Trop. Med. Hyg.* **71S**, 1–15.
2. Oaks, S.C., Mitchell, V.S., Jr, Pearson, G.W. & Carpenter, C.C.J., eds (1991) *Malaria: Obstacles and Opportunities*. A report of the committee for the study on malaria prevention and control: Status review and alternate strategies. Division of International Health, Institute of Medicine, National Academy, Washington, DC.
3. White, N.J. (1998) Drug resistance in malaria. *Br. Med. Bull.* **54**, 703–715.
4. Jiang, S., Prigge, S.T., Wei, L., Gao, Y.E., Hudson, T.H, Gerena, L., Dame, J.B. & Kyle, D.E. (2001) New class of small nonpeptidyl compounds blocks *Plasmodium falciparum* development in vitro by inhibiting plasmepsins. *Antimicrob. Agents Chemother.* **45**, 2577–2584.
5. Rosenthal, P.J., McKerrow, J.H., Aikawa, M., Nagasawa, H. & Leech, J.H. (1988) A malarial cysteine proteinase is necessary for hemoglobin degradation by *Plasmodium falciparum*. *J. Clin. Invest.* **82**, 1560–1566.
6. Eggleson, K.K., Duffin, K.L. & Goldberg, D.E. (1999) Identification and characterization of falcilysin, a metallopeptidase involved in hemoglobin catabolism within the malaria parasite *Plasmodium falciparum*. *J. Biol. Chem.* **274**, 32411–32417.
7. Francis, S.E., Gluzman, I.Y., Oksman, A., Knickerbocker, A., Mueller, R., Bryant, M., Sherman, D.R., Russell, D.G. & Goldberg, D.E. (1994) Molecular characterization and inhibition of *Plasmodium falciparum* aspartic hemogloinase. *EMBO J.* **13**, 306–317.
8. Berry, C., Humphreys, J., Matharu, P., Granger, R., Horrocks, P., Moon, R.P., Certa, U., Ridley, R.G., Bur, D. & Kay, J. (1999) A distinct member of the aspartic proteinase gene family from the human malaria parasite *Plasmodium falciparum*. *FEBS Lett.* **447**, 149–154.
9. Banerjee, R., Liu, J., Beatty, W., Klemba, M. & Goldberg, D.E. (2002) Four plasmepsins are active in the *Plasmodium falciparum* food vacuole, including a protease with an active site histidine. *Proc. Natl. Acad. Sci. USA* **99**, 990–995.
10. Coombs, G.H., Goldberg, D.E., Klemba, M., Berry, C., Kay, J. & Mottram, J.C. (2001) Aspartic proteases of *Plasmodium falciparum* and other parasitic protozoa as drug targets. *Trends Parasitol.* **17**, 532–537.
11. Noteberg, D., Hamelink, E., Hulten, J., Wahlgren, M., Vrang, L., Samuelsson, B. & Hallberg, A. (2003) Design and synthesis of plasmepsin I and plasmepsin II inhibitors with activity in *Plasmodium falciparum*-infected cultured human erythrocytes. *J. Med. Chem.* **46**, 734–746.
12. Johansson, P.-O., Lindberg, J., Blackman, M.J., Kvarnstrom, I., Vrang, L., Hamelink, E., Hallberg, A., Rosenquist, A. & Samuelsson, B. (2005) Design and synthesis of potent inhibitors of plasmepsin I and II: X-ray crystal structure of inhibitor in complex with plasmepsin II. *J. Med. Chem.* **48**, 4400–4409.
13. Asojo, O.A., Gulnik, S.V., Afonina, E., Yu, B., Ellman, J.A., Haque, T.S. & Silva, A.M. (2003) Novel uncomplexed and complxed structures of plasmepsin II, an aspartic protease from *Plasmodium falciparum*. *J. Mol. Biol.* **327**, 173–181.
14. Mueller, R., Huerzeler, M. & Boss, C. (2003) Synthesis of Plasmepsin II inhibitors-Potential Antimalarial agents. *Molecules* **8**, 556–564.
15. Asojo, O.A., Afonina, E., Gulnik, S.V., Yu, B., Erickson, J.W., Randad, R., Medjahed, D. & Silva, A.M. (2002) Structures of Ser205 mutant plasmepsin II from *Plasmodium falciparum* at 1.8 Å in complex with the inhibitors rs367 and rs370. *Acta. cryst.* **D58**, 2001–2008.
16. Dahlgren, A., Kvarnstrom, I., Vrang, L., Hamelink, E., Hallberg, A., Rosenquist & Samuelsson, A.B. (2003) New inhibitors of the malaria aspartyl proteases plasmepsin I and II. *Bioorg. Med. Chem.* **11**, 3423–3437.
17. Ersmark, K., Feierberg, I., Bjelic, S., Hamelink, E., Hackett, F., Blackman, M.J., Hulten, J., Samuelsson, B., Aqvist, J. & Hallberg, A. (2004) Potent inhibitors of the *Plasmodium falciparum* enzymes plasmepsins I and II devoid of cathepsin D inhibitory activity. *J. Med. Chem.* **47**, 110–122.
18. Silva, A.M., Lee, A.Y., Gulnik, S.V., Majer, P., Collins, J., Bhat, T.N., Collins, P.J., Cachau, R.E., Luker, K.E., Gluzman, I.Y., Francis, S.E., Oksman, A., Goldberg, D.E. & Erickson, J.W. (1996) Structure and inhibition of plasmepsin II, a hemoglobin degrading enzyme from *Plasmodium falciparum*. *Proc. Natl. Acad. Sci. USA.* **93**, 10034–10039.
19. Prade, L., Jones, A.F., Boss, C., Richard-Bildstein, S., Meyer, S., Binkert, C. & Bur, D. (2005) X-ray structure of plasmepsin II complexed with a potent achiral inhibitor. *J. Biol. Chem.* **280**, 23837–23843.
20. Trager, W. & Jenson, J.B. (1976) Human malaria parasites in continuous culture. *Science* **193**, 673–675.
21. Lambros, C. & Vanderberg, J. (1979) Synchronization of *Plasmodium falciparum* erythrocytic stages in culture. *J. Parasitol.* **65**, 418–420.
22. Ancelin, M.L., Calas, M., Bompart, J., Cordina, G., Martin, D., Ben Bari, M., Jei, T., Druilhe, P. & Vial, H.J. (1998) Antimalarial activity of 77 phospholipid polar head analogs: close correlation between inhibition of phospholipid metabolism and *in vitro Plasmodium falciparum* growth. *Blood* **91**, 1426–1437.
23. Sheldrick, G.M. (1997) *SHELXS* 97, Program for Automatic Solution of Crystal Structures & SHELXL 97, Program for crystal structure refinement. University of Gottingen, Gottingen, Germany.
24. Tripos Associates, Inc. (1999) *Program SYBYL*. Tripos Associates, Inc., St Louis, MO.
25. Morris, G.M., Goodshell, D.S., Halliday, R.S., Huey, R., Hart, W.E., Belew, R.K. & Olson, A.J. (1998) Automated docking using a Lamarckian genetic algorithm and empirical binding free energy function. *J. Comp. Chem.* **19**, 1639–1662.